Geodesics Between 3D Closed Curves Using Path-Straightening

Eric Klassen[1] and Anuj Srivastava[2]

[1] Department of Mathematics, Florida State University, Tallahassee, FL 32306
[2] Department of Statistics, Florida State University, Tallahassee, FL 32306

Abstract. In order to analyze shapes of continuous curves in $\mathbb{R}^3$, we parameterize them by arc-length and represent them as curves on a unit two-sphere. We identify the subset denoting the closed curves, and study its differential geometry. To compute geodesics between any two such curves, we connect them with an arbitrary path, and then iteratively straighten this path using the gradient of an energy associated with this path. The limiting path of this path-straightening approach is a geodesic. Next, we consider the shape space of these curves by removing shape-preserving transformations such as rotation and re-parametrization. To construct a geodesic in this shape space, we construct the shortest geodesic between the all possible transformations of the two end shapes; this is accomplished using an iterative procedure. We provide step-by-step descriptions of all the procedures, and demonstrate them with simple examples.

1 Introduction

In recent years, there has been an increasing interest in analyzing shapes of objects. This research is motivated in part by the fact that shapes of objects form an important feature for characterizing them, with applications in recognition, tracking, and classification. For instance, shapes of boundaries of objects in images can be used to short-list possible objects present in those images. Also, shape has been used as a feature in image retrieval [14, 4, 6]. Shape analysis in image=based applications is often restricted to shapes of planar curves [19, 11, 8]; these curves can come, for example, from the boundaries of objects in 2D images. Shapes have also been used for medical diagnosis using non-invasive imaging techniques. Shapes, or growths of shapes, are often used to determine normailty/abnormalty of anatomical parts in computational anatomy [5]. A fundamental tool, central to any differential-geometric analysis of shapes, is the construction of a geodesic path path between any two given shapes in a pre-determined shape space. This tool can lead to a full statistical analysis – computation of means, covariances, tangent-space probability models – on shape spaces. As an example, the construction of geodesics and their use in statistical analysis of shapes of 2D curves is demonstrated in [8].

Although analysis of planar curves are useful in certain image understanding problems, a more general issue is to study and compare shapes of objects in 3D. Since most objects of interest are 3D objects, and 3D observations of objects

A. Leonardis, H. Bischof, and A. Pinz (Eds.): ECCV 2006, Part I, LNCS 3951, pp. 95–106, 2006.

using laser scans are becoming readily available, an important goal is to analyze shapes of two-dimensional surfaces in $\mathbb{R}^3$. In particular, given surfaces of two objects, the task is to quantify differences between their shapes. A differential-geometric analysis of shapes of surfaces, akin to the analysis of planar curves discussed above, remains a difficult and an unsolved problem. To our knowledge, there is no explicit method in the literature for computing geodesic between 3D closed curves. Several approximate methods have been pursued over the last few years. For example, the papers [16, 15] use histograms of distances on surfaces to represent and compare objects. Another approximate approach that has been suggested in recent years is to represent surfaces with a finite number of level curves, and then compare shapes of surfaces by comparing shapes of corresponding level curves [18]. Since these level curves can potentially be 3D curves [2], this approach requires a technique for comparing shapes of closed curves in $\mathbb{R}^3$. However, past research on geometric treatment of shapes of curves was restricted mainly to planar curves and a similar differential-geometric approach for comparing shapes of closed, continuous curves in $\mathbb{R}^3$ is not present in the literature, to the best of our knowledge.

In this paper, we present a differential-geometric technique for constructing geodesic paths between shapes of arbitrary two closed, continuous curves in $\mathbb{R}^3$. Given two curves p_0 and p_1, our basic approach is to: (i) define a shape space of all parameterized, closed curves in $\mathbb{R}^3$, (ii) construct an initial path connecting p_0 and p_1 in this space, and (iii) iteratively straighten this path until it becomes a geodesic path. This iteration is performed to minimize an energy associated with a path, and flows that minimize that energy are called *path-straightening* flows [9, 10], and more recently in [3, 13]. This methodology is quite different from the approach used in [8] where a shooting method was used to find geodesic paths between shapes. In a shooting method, one searches for a tangent direction at the first shape such that a geodesic *shot* in that direction reaches the target shape in a unit time. This search is based on adjusting the shooting direction in such a way that the miss function, defined as an extrinsic distance between the shape reached and the target shape, goes to zero. Intuitively, a path-straightening flow is expected to perform better than a shooting method for the following reasons:

1. While shooting, in principle, one can get stuck in a local minima of the miss function that is bounded away from zero. In other words, the resulting geodesic may not reach the target shape. In the path-straightening method, by construction, the geodesic always reaches the target shape.
2. Since the shooting is performed using numerical techniques, i.e. using numerical gradient of the miss function, these iterations can become unstable if the manifold is sharply curved near the target shape. A path-straightening approach, on the other hand, is numerically more stable as it uses the gradient of path length.

We will develop a path-straightening approach to computing geodesics in $\mathcal{C}$, the space of all closed curves in $\mathbb{R}^3$. Here we do not take into account the shapes of these curves, and the fact that many curves have the same shape. In future, we will define a shape space, as a quotient space of $\mathcal{C}$, and derive algorithms for computing geodesics between elements of this shape space.

The rest of this paper is organized as follows. In Section 2, we present a representation of closed curves, and analyze the geometry of $\mathcal{C}$, the space of such curves. Section 3 presents a formal discussion on the construction of path-straightening flows on $\mathcal{C}$, followed by algorithms for computer implementations in Section 4. Section 5 presents some illustrative examples on computing geodesic paths in $\mathcal{C}$. The paper ends with a summary in Section 6.

2 Geometry of Shapes and Shape Spaces

In this section we introduce a geometric representation of curves that underlies our construction of geodesics and the resulting analysis of shapes.

2.1 Representations of Closed Curves

Let $p : [0, 2\pi) \mapsto \mathbb{R}^3$ be a curve of length 2π, parameterized by the arc length. In this paper we will assume p to be piecewise C^1. For $v(s) \equiv \dot{p}(s) \in \mathbb{R}^3$, we have $\|v(s)\| = 1$ for all $s \in [0, 2\pi)$, in view of the arc-length parametrization. Here $\| \cdot \|$ denotes the Euclidean norm in $\mathbb{R}^3$. Note that the restriction to arc-length parametrization can be relaxed, as is done in [12], resulting in elastic-string models, but is not pursued in this paper. The function v is called the *direction function* of p and itself can be viewed as a curve on the unit sphere $\mathbb{S}^2$, i.e. $v : [0, 2\pi) \mapsto \mathbb{S}^2$. Shown in Figure 1(a) is an illustration of this idea where a closed curve p on $\mathbb{R}^3$ is represented by a curve v in $\mathbb{S}^2$. We will use the direction function v to represent the curve p . Let $\mathcal{P}$ be the set of all such direction functions, $\mathcal{P} = \{v | v : [0, 2\pi) \mapsto \mathbb{S}^2\}$. Since we are interested in *closed* curves, we establish that set as follows. Define a map $\phi : \mathcal{P} \mapsto \mathbb{R}^3$ by $\phi(v) = \int_0^{2\pi} v(s) ds$, and define $\mathcal{C} = \phi^{-1}(0) \equiv \{v \in \mathcal{P} | \phi(v) = 0\} \quad \subset \mathcal{P}$. It is easy to see that $\mathcal{C}$ is the set of all closed curves in $\mathbb{R}^3$. In the next section we will study the geometry of $\mathcal{C}$ in order to develop tools for shape analysis.

First, we introduce some notation for studying geometry of $\mathbb{S}^2$. Recall that geodesics on $\mathbb{S}^2$ are great circles, and we have analytical expressions for computing them. The geodesic on $\mathbb{S}^2$ starting at a point $x \in \mathbb{S}^2$ in the tangent direction $a \in T_x(\mathbb{S}^2)$ is given by:

$$\chi_t(x; a) = \cos(t\|a\|)x + \frac{\sin(t\|a\|)}{\|a\|} a \ . \tag{1}$$

χ_t will be used frequently in this paper to denote geodesics, or great circles, on $\mathbb{S}^2$. Another item that we need relates to the rotation of tangent vectors on $\mathbb{S}^2$. Let x_1 and x_2 be two elements in $\mathbb{S}^2$, and let a be a tangent to $\mathbb{S}^2$ at x_1. Then, a vector defined as:

$$\pi(a; x_1, x_2) = \begin{cases} a - (2(a \cdot x_2)/(\|x_1 + x_2\|^2))(x_1 + x_2) & \text{if } \ x_1 \neq -x_2 \\ -a & \text{if } \ x_1 = -x_2 \end{cases} \tag{2}$$

is the rotation of a to x_2 so that it is now tangent to $\mathbb{S}^2$ at x_2. Here, $(a \cdot b)$ denotes the Euclidean inner product of $a, b \in \mathbb{R}^3$. $\pi(\cdot, x_1, x_2) : T_{x_1}(\mathbb{S}^1) \mapsto T_{x_2}(\mathbb{S}^1)$ is a rotation map that takes a tangent vector from x_1 to x_2; in differential geometry this is also called the *parallel transport* along the geodesic from x_1 to x_2.

2.2 Geometry of $\mathcal{C}$

To develop a geometric framework for analyzing elements of $\mathcal{C}$, we would like understand its tangent bundle and to impose a Riemannian structure on it. First, we focus on the set $\mathcal{P}$. On any point $v \in \mathcal{P}$, what form does a tangent f to $\mathcal{P}$ takes? This tangent f can be derived by constructing a one-parameter flow passing through v, and by computing its velocity at v. Since v is also a curve on $\mathbb{S}^2$, the tangent f can also be viewed as a field of vectors tangent to $\mathbb{S}^2$ on v. This idea is illustrated pictorially in Figure 1(b). We will interchangeably refer to f as a tangent vector on $\mathcal{P}$ and a tangent vector field on points along $v \subset \mathbb{S}^2$. The space of all such tangent vectors, denoted by $T_v(\mathcal{P})$, is given by: $T_v(\mathcal{P}) = \{f | f : [0, 2\pi) \mapsto \mathbb{R}^3, (f(s) \cdot v(s)) = 0, \ \forall s\}$. $f(s)$ and $v(s)$ are vectors in $\mathbb{R}^3$. Let $f \in T_v(\mathcal{P})$ be a vector field on v such that it is also tangent to $\mathcal{C}$. It can be shown that f satisfies $\int f(s)ds = 0$. That is,

$$T_v(\mathcal{C}) = \{f | f : [0, 2\pi) \mapsto \mathbb{R}^3, \ \forall s, \ (f(s) \cdot v(s)) = 0, \ \int_0^{2\pi} f(s)ds = 0\} \ . \qquad (3)$$

To see that, let $\alpha(t)$ be a path in $\mathcal{C}$ such that $\alpha(0) = v$. Since $\alpha(t) \in \mathcal{C}$, we have $\int_0^{2\pi} \alpha(t)(s)ds = 0$, for all t. Taking the derivative with respect to t and setting $t = 0$, we get $\int_0^{2\pi} \dot{\alpha}(0)(s)ds = 0$. For every tangent vector f at v there is a corresponding flow α, such that $f = \dot{\alpha}(0)$, and therefore, this property is satisfied by all tangent vectors.

Riemannian Structure: To impose a Riemannian structure on $\mathcal{P}$, we will assume the following inner product on $T_v(\mathcal{P})$: for $f, g \in T_v(\mathcal{P})$, $\langle f, g \rangle = \int_0^{2\pi} (f(s) \cdot g(s))ds$.

Consider the linear mapping $d\phi_v : T_v(\mathcal{P}) \mapsto \mathbb{R}^3$ defined by $d\phi_v(f) = \int_0^{2\pi} f(s)ds$. Similar to the argument in [13], it can be shown that $d\phi_v$ is surjective,

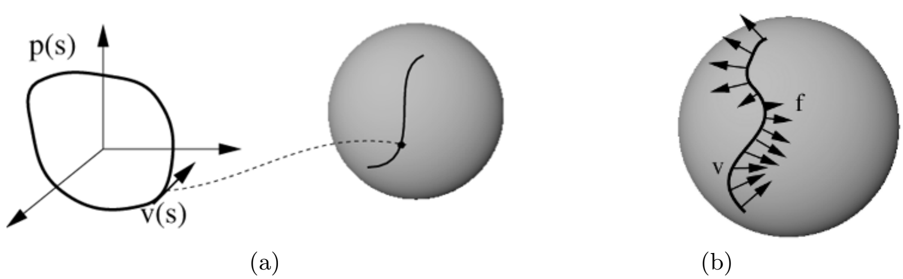

Fig. 1. (a): A closed curve in $\mathbb{R}^3$ is denoted by a curve on $\mathbb{S}^2$. (b): For a curve v on $\mathbb{S}^2$, f is vector field to $\mathbb{S}^2$ on v.

as long as $v([0, 2\pi))$ is not contained in a one-dimensional subspace of $\mathbb{R}^3$, and therefore $\mathcal{C}$ is a co-dimension three submanifold of $\mathcal{P}$. The adjoint of $d\phi_v$, $d\phi_v^* : \mathbb{R}^3 \to T_v(\mathcal{P})$ is the unique linear transformation with the property that for all $f \in T_v(\mathcal{P})$ and $w \in \mathbb{R}^3$, $(d\phi_v(f) \cdot w) = \langle f, d\phi_v^*(w)\rangle$. Mathematically, this adjoint is given by $d\phi_v^*(w) \equiv f$ such that $f(s) = w - (w \cdot v(s))v(s)$. In other words, $d\phi_v^*$ takes a vector w in $\mathbb{R}^3$ and forms a tangent vector-field on v by making w perpendicular to $v(s)$ for all s (or by projecting w onto the tangent space $T_{v(s)}(\mathbb{S}^2)$ for each s). This formula makes explicit the role of v in definition of $d\phi_v^*$.

With this framework, we develop tools for projecting $v \in \mathcal{P}$ into $\mathcal{C}$. Also, we derive a mechanism for projecting $f \in T_v(\mathcal{P})$ into $T_v(\mathcal{C})$. For details we refer to a larger paper [7].

3 Path-Straightening Flows in $\mathcal{C}$

Now we present our approach for constructing geodesic flows on $\mathcal{C}$. This approach is based on the use of path-straightening flows. That is, we connect the two given shapes by an arbitrary path in $\mathcal{C}$, and then iteratively straighten it, or shorten it, using a gradient approach till we reach a fixed point. The fixed point of this iterative procedure becomes the desired geodesic path. In this section we present formal mathematical ideas, followed by computer implementations in the next section.

For any two closed curves, denoted by v_0 and v_1 in $\mathcal{C}$, we are interested in finding a geodesic path between them in $\mathcal{C}$. Our approach is to start with any path $\alpha(t)$ connecting v_0 and v_1. That is $\alpha : [0, 1] \mapsto \mathcal{C}$ such that $\alpha(0) = v_0$ and $\alpha(1) = v_1$. Then, we iteratively "straighten" α till it achieves a local minimum of the energy: $E(\alpha) \equiv \frac{1}{2} \int_0^1 (\frac{d\alpha}{dt}(t). \frac{d\alpha}{dt}(t))dt$. It can be shown that a local minimum of E is a geodesic on $\mathcal{C}$. However, it is possible that there are multiple geodesics between a given pair of curves, and a local minimum of E may not correspond to the shortest of all geodesics. Therefore, this approach has the limitation that it finds a geodesic between a given pair but may not reach the shortest geodesic. One can use certain stochastic techniques to increase the probability of reaching the shortest geodesic but these are not explored in this paper.

Let $\mathcal{H}$ be the set of all paths in $\mathcal{C}$, parameterized by $t \in [0, 1]$, and $\mathcal{H}_0$ be the subset of $\mathcal{H}$ of paths that start at v_0 and end at v_1. The tangent spaces of $\mathcal{H}$ and $\mathcal{H}_0$ are: $T_\alpha(\mathcal{H}) = \{w | \; \forall t \in [0, 1], w(t) \in T_{\alpha(t)}(\mathcal{C})\}$, where $T_{\alpha(t)}(\mathcal{C})$ is as specified in Eqn. 3, and $T_\alpha(\mathcal{H}_0) = \{w \in T_\alpha(\mathcal{H}) | w(0) = w(1) = 0\}$. To understand this space, consider a path $\alpha \in \mathcal{H}_0$ and an element $w \in T_\alpha(\mathcal{H}_0)$. Recall that for any t, $\alpha(t)$ is also a curve on $\mathbb{S}^2$, which in turn corresponds to a closed curve in $\mathbb{R}^3$. Now, w is path of vector fields such that for any $t \in [0, 1]$, $w(t)$ is a tangent vector field restricted to the curve $\alpha(t)$ on $\mathbb{S}^2$. That is, $w(t)(s)$ is a vector tangent to $\mathbb{S}^2$ at the point $\alpha(t)(s)$. Furthermore, $\int_0^{2\pi} w(t)(s)ds = 0$ for all $t \in [0, 1]$. Our study of paths on $\mathcal{H}$ requires the use of covariant derivatives and integrals of vector fields along these paths.

Definition 1 (Covariant Derivative, [1](pg. 309)). *For a given path $\alpha \in \mathcal{H}$ and a vector field $w \in T_\alpha(\mathcal{H})$, one defines the covariant derivative of w along α to be the vector field obtained by projecting $\frac{dw}{dt}(t)$ onto the tangent space $T_{\alpha(t)}(\mathcal{C})$, for all t. It is denoted by $\frac{Dw}{dt}$.*

Similarly, a vector field $u \in T_\alpha(\mathcal{H})$ is called the *covariant integral* of w along α if the covariant derivative of u is w, i.e. $\frac{Du}{dt} = w(t)$.

To make $\mathcal{H}$ a Riemannian manifold, we use the Palais metric [17]: for w_1, $w_2 \in T_\alpha(\mathcal{H})$, $\langle\langle w_1, w_2\rangle\rangle = \langle w_1(0), w_2(0)\rangle + \int_0^1 \left\langle \frac{Dw_1}{dt}(t), \frac{Dw_2}{dt}(t)\right\rangle dt$, where Dw/dt denotes the vector field along α which is the covariant derivative of w. With respect to the Palais metric, $T_\alpha(\mathcal{H}_0)$ is a closed linear subspace of $T_\alpha(\mathcal{H})$, and $\mathcal{H}_0$ is a closed subspace of $\mathcal{H}$.

Our goal is to find a minimizer of E in $\mathcal{H}_0$, and we will use a gradient flow to minimize E. Therefore, we wish to find the gradient of E in $T_\alpha(\mathcal{H}_0)$. To do this, we first find the gradient of E in $T_\alpha(\mathcal{H})$ and then project it into $T_\alpha(\mathcal{H}_0)$.

Theorem 1. *The gradient vector of E in $T_\alpha(\mathcal{H})$ is given by a vector field q such that $\frac{Dq}{dt} = \frac{d\alpha}{dt}$ and $q(0) = 0$. In other words, q is the covariant integral of $\frac{d\alpha}{dt}$ with zero initial value at $t = 0$.*

Proof: Refer to a more detailed paper [7].

Given $\frac{d\alpha}{dt}$, the vector field q is obtained using numerical techniques for covariant integration, as described in the next section. Next, we want to project tangent field $q \in T_\alpha(\mathcal{H})$ to the space $T_\alpha(\mathcal{H}_0)$.

Definition 2 (Covariantly Constant). *A vector field w along the path α is called covariantly constant if Dw/dt is zero at all points on α.*

Definition 3 (Geodesic). *A path is called a geodesic if its velocity vector field is covariantly constant. That is, α is a geodesic if $\frac{D}{dt}(\frac{d\alpha}{dt}) = 0$ for all t.*

Definition 4 (Covariantly Linear). *A vector field w along the path α is called covariantly linear if Dw/dt is a covariantly constant vector field.*

Lemma 1. *The orthogonal complement of $T_\alpha(\mathcal{H}_0)$ in $T_\alpha(\mathcal{H})$ is the space of all covariantly linear vector fields w along α.*

Definition 5 (Parallel Translation). *A vector field u is called the forward parallel translation of a tangent vector $w \in T_{\alpha(0)}(\mathcal{C})$, along α, if and only if $u(0) = w$ and $\frac{Du(t)}{dt} = 0$ for all $t \in [0, 1]$.*

Similarly, u is called the backward parallel translation of a tangent vector $w \in T_{\alpha(1)}(\mathcal{C})$, along α, when for $\tilde{\alpha}(t) \equiv \alpha(1-t)$, u is the forward parallel translation of w along $\tilde{\alpha}$.

It must be noted that parallel translations, forward or backward, lead to vector fields that are covariantly constant.

According to Lemma 1, to project the gradient q into $T_\alpha(\mathcal{H}_0)$, we simply need to subtract off a covariantly linear vector field which agrees with q at $t = 0$ and $t = 1$. Clearly, the correct covariantly linear field is simply $t\tilde{q}(t)$, where $\tilde{q}(t)$ is the covariantly constant field obtained by parallel translating $q(1)$ backwards along α. Hence, we have proved following theorems.

Theorem 2. *Let $\alpha : [0,1] \mapsto \mathcal{C}$ be a path, $\alpha \in \mathcal{H}_0$. Then, with respect to the Palais metric:*

1. *The gradient of the energy function E on $\mathcal{H}$ is the vector field q along α satisfying $q(0) = 0$ and $\frac{Dq}{dt} = \frac{d\alpha}{dt}$.*
2. *The gradient of the energy function E restricted to $\mathcal{H}_0$ is $w(t) = q(t) - t\tilde{q}(t)$, where q is the vector field defined in the previous item, and $\tilde{q}$ is the vector field obtained by parallel translating $q(1)$ backwards along α.*

Theorem 3. *For a given pair v_0, $v_1 \in \mathcal{C}$, a critical point of E on $\mathcal{H}_0$ is a geodesic on $\mathcal{C}$ connecting v_0 and v_1.*

4 Computer Implementations

In this section, we provide step-by-step details for different procedures mentioned in the last section. In particular, we provide algorithms for: (i) finding the direction vector representation of a given closed curve p, (ii) given any two closed curves, v_0 and v_1, initializing a path α connecting them in $\mathcal{C}$, (iii) computing the velocity vector $\frac{d\alpha}{dt}$ for a given path α, (iv) computing the covariant derivative q of $\frac{d\alpha}{dt}$, (v) computing the backward parallel transport $\tilde{q}$ of $q(1)$, and (vi) updating the path α along the gradient direction given by the vector field w. We explain these procedures one by one next.

1. **Direction Function Representation of closed curves:** The first computational step in our analysis is to find an element of $\mathcal{C}$ for a given 3D curve. Let $x_i \in \mathbb{R}^3$, $i = 1, \ldots, m$ be a given order set of samples on a 3D curve. and we want to re-sample this curve using n uniform samples as follows:

   Subroutine 1 (Uniform Re-sampling of Curve)

   set $x_{m+1} = x_1$
   compute $\rho_i = \|x_{i+1} - x_i\|$, $i = 1, \ldots, m$
   while standard-deviation$(\{\rho_i\}) > \epsilon$
       $s_i = \sum_{j=1}^{i} \rho_j$, $i = 1, \ldots, m$
       $t = ([1:n]/n)s_m$
       $k_j = \mathrm{argmin}_i(s_i \geq t_j)$, $j = 1, \ldots, n$
       $y_1 = x_1$
       for $j = 1, \ldots, n-1$
           $y_{j+1} = ((t_j - x_{k_j-1})x_{k_j+1} + (x_{k_j} - t_j)x_{k_j})/(x_{k_j+1} - x_{k_j})$
           $w_j = y_{j+1} - y_j$, *and* $v_j = \frac{w_j}{\|w_j\|}$, $\rho_j = \|w_j\|$,
       end j
       set $m = n$ *and* $x = y$.
   end while
   project v *into* $\mathcal{C}$

   Shown in Figure 2 is an example. The given curve with $m = 200$ is shown in the left panel; it is re-sampled repeatedly for $n = 30$ with results shown

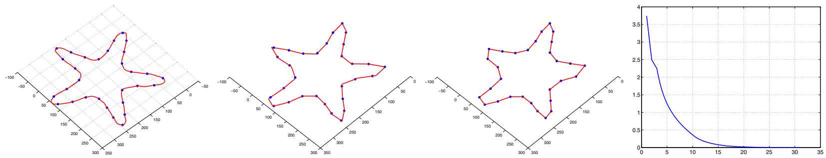

Fig. 2. Resampling the piecewise-linear curve formed by the given set of points using Subroutine 1. Right: evolution of standard deviation of distances between resampled points.

in next two panels. To show that points become increasingly uniform, we show the standard deviation of ρ_js at every iteration. A standard deviation of zero implies that the points are uniformly spaced.

2. **Initialize the path** α**:** Given v_0 and v_1 in $\mathcal{C}$, we want to form a path $\alpha : [0,1] \mapsto \mathcal{C}$ such that $\alpha(0) = v_0$ and $\alpha(1) = v_1$. There are several ways of doing this. One is to form 3D coordinates p_0 and p_1, respectively, associated with the two shapes, and connect $p_0(s)$ and $p_1(s)$ linearly, for all s, using $p_t(s) = tp_1(s) + (1-t)p_0(s)$. The intermediate curves are neither uniformly sampled nor closed. We can use Subroutine 1 to re-sample them uniformly and to close them. The other idea is to use the fact that $v_0(s), v_1(s) \in \mathbb{S}^2$, and construct a path in $\mathbb{S}^2$ from one point to another, parameterized by t. We summarize this idea in the following subroutine.

   Subroutine 2 (Initialize a path α**)**
   for all $s \in [0, 2\pi]$
   define $\theta(s) = \cos^{-1}(v_0(s) \cdot v_1(s))$
   define $f(s) = v_1(s) - (v_0(s) \cdot v_1(s))v_0(s)$, *and* $f(s) = \theta(s)f(s)/\|f(s)\|$.
   end s
   for all $t \in [0, 1]$
   for all $s \in [0, 2\pi)$
   define $\alpha(t)(s) = \chi_1(v_0(s); f(s))$
   end s
   project $\alpha(t)$ *into* $\mathcal{C}$
   end t

   In case $v_0(s)$ and $v_1(s)$ are antipodal points on $\mathbb{S}^2$, and thus $f(s) = 0$, one can arbitrarily choose a path connecting them on the sphere. That is, choose any $f(s) \in T_{v_0(s)}(\mathbb{S}^1)$ of length $\theta(s)$. This situation rarely occurs in practical situations.
3. **Vector Field** $\frac{d\alpha}{dt}$**:** In order to compute the gradient of E in $T_\alpha(\mathcal{H})$, we first need to compute the path velocity $\frac{d\alpha}{dt}$. For a continuous path $\frac{d\alpha}{dt}(t)$ automatically lies in $T_{\alpha(t)}(\mathcal{C})$, but in the discrete case one has to ensure this property using additional steps. This process uses the approximation $x'(t) \approx (x(t) - x(t-\epsilon))/\epsilon$, modified to account for the nonlinearity of $\mathcal{C}$. Let the interval $[0,1]$ be divided into k uniform bins. The procedure for computing $\frac{d\alpha}{dt}$ at these discrete times is summarized next.

Subroutine 3 (Computation of $\frac{d\alpha}{dt}$ along α)

for $\tau = 1, \dots, k$
  for all $s \in [0, 2\pi)$
    $\theta(s) = k\cos^{-1}(\alpha(\frac{\tau}{k})(s) \cdot \alpha(\frac{\tau-1}{k})(s))$
    $f(s) = -\alpha(\frac{\tau-1}{k})(s) + (\alpha(\frac{\tau-1}{k})(s) \cdot \alpha(\frac{\tau}{k})(s))\alpha(\frac{\tau}{k})(s)$
    $\frac{d\alpha}{dt}(\frac{\tau}{k})(s) = \theta(s)f(s)/\|f(s)\|$.
  end s
  project $\frac{d\alpha}{dt}(\frac{\tau}{k})$ *into* $T_{\alpha(\frac{\tau}{k})}(\mathcal{C})$
end τ.

Now we have a vector field $\frac{d\alpha}{dt} \in T_\alpha(\mathcal{H})$ along a given path $\alpha \in \mathcal{H}$.

4. **Computation of Vector field q:** We seek a vector field q such that $q(0) = 0$ and $\frac{Dq}{dt} = \frac{d\alpha}{dt}$. In other words, q is the covariant integral of the vector field $\frac{d\alpha}{dt}$.

Subroutine 4 (Covariance Integration of $\frac{d\alpha}{dt}$ to form q)

for $\tau = 0, 1, 2, \dots, k-1$,
  for all s
    define $q^{\|}(\frac{\tau}{k})(s) = \pi(q(\frac{\tau}{k})(s); \alpha(\frac{\tau}{k})(s), \alpha(\frac{\tau+1}{k})(s))$.
    (π is defined in Eqn. 2)
    set $q(\frac{\tau+1}{k})(s) = \frac{1}{k}\frac{d\alpha}{dt}(\frac{\tau+1}{k})(s) + q^{\|}(\frac{\tau}{k})(s)$.
  end s
end τ

$q^{\|}(\frac{\tau}{k})$ is the parallel transport of $q(\frac{\tau}{k})$ from $T_{\alpha(\frac{\tau}{k})}(\mathcal{C})$ to $T_{\alpha(\frac{\tau+1}{k})}(\mathcal{C})$. This subroutine results in the gradient vector field $\{q(\frac{\tau}{k}) \in T_{\alpha(\frac{\tau}{k})}(\mathcal{C}) | \tau = 1, \dots, k\}$.

5. **Covariant Vector Field $\tilde{q}$:** Given $q(1)$, we need to find a vector field $\tilde{q}$ along the path α in $\mathcal{C}$ that is the backward parallel transport of $q(1)$. We have already computed the points $\alpha(0), \alpha(1/k), \alpha(2/k), \dots, \alpha(1)$. Each $\alpha(\frac{\tau}{k})$ is an element of $\mathcal{C}$, i.e. it is a curve on $\mathbb{S}^2$. We will perform the backward parallel transport iteratively, as follows.

Subroutine 5 (Backward Parallel Transport)

set $\tilde{q}(1) = q(1)$
let $l = (\langle q(1), q(1)\rangle)^{1/2}$
for $\tau = k-1, k-2, \dots, 3, 2$
  for all $s \in [0, 2\pi)$
    $\tilde{q}(\frac{\tau}{k})(s) = \pi(\tilde{q}(\frac{\tau+1}{k})(s); \alpha(\frac{\tau+1}{k})(s), \alpha(\frac{\tau}{k})(s))$
  end s
  project $\tilde{q}(\frac{\tau}{k})$ *into* $T_{\alpha(\frac{\tau}{k})}(\mathcal{C})$
  let $l_1 = (\langle \tilde{q}(\frac{\tau}{k}), \tilde{q}(\frac{\tau}{k})\rangle)^{1/2}$
  set $\tilde{q}(\frac{\tau}{k}) = \tilde{q}(\frac{\tau}{k})l/l_1$;
end τ

6. **Gradient of E:** With the computation of q and $\tilde{q}$ along the path α, the gradient vector field of E is given by: for any $\tau \in \{0, 1, \dots, k\}$ and $s \in [0, 2\pi)$

$$w(\frac{\tau}{k})(s) \equiv (q(\frac{\tau}{k})(s) - (\frac{\tau}{k})\tilde{q}(\frac{\tau}{k})(s)) \quad \in T_{\alpha(\frac{\tau}{k})(s)}(\mathbb{S}^2) \ . \tag{4}$$

7. **Update in Gradient Direction:** Now that we have computed the gradient vector field w on the current path α, we update this path in the direction given by w: for $\tau = 1, 2, \ldots, k$ and $s \in [0, 2\pi)$,

$$\alpha(\frac{\tau}{k})(s) = \chi_1(\alpha(\frac{\tau}{k})(s); w(\frac{\tau}{k})(s)) \ . \quad (5)$$

Now we summarize the algorithm to compute a geodesic path between any two given closed curves in $\mathbb{R}^3$. We assume that the curves are available in form of sampled points on these curves.

Algorithm 1 (Find a geodesic between two curves in $\mathcal{C}$)

1. *Compute the representations of each curve in $\mathcal{C}$ using Subroutine 1. Denote these elements by v_0 and v_1, respectively.*
2. *Initialize a path α between v_0 and v_1 using Subroutine 2.*
3. *Compute the velocity vector field $\frac{d\alpha}{dt}$ along the path α using Subroutine 3.*
4. *Compute the covariant integral of $\frac{d\alpha}{dt}$, denoted by q, using Subroutine 4. If $\sum_{\tau=1}^{k} \langle \frac{d\alpha}{dt}(\tau), \frac{d\alpha}{dt}(\tau) \rangle$ is small, then stop. Else, continue to the next step.*
5. *Compute the backward parallel transport of the vector $q(1)$ along α using the Subroutine 5.*
6. *Compute the full gradient vector field of the energy E along the path α, denoted by w, using Eqn. 4.*
7. *Update α using Eqn. 5. Return to Step 3.*

The desired geodesic path is given by the resulting α, and its length is given by $d_{\mathcal{C}}(v_0, v_1) = \sum_{\tau=1}^{k} (\langle \frac{d\alpha}{dt}(\frac{\tau}{k}), \frac{d\alpha}{dt}(\frac{\tau}{k}) \rangle)^{1/2}$. For a later use, we highlight $\frac{d\alpha}{dt}(0)$ as the initial velocity vector in $T_{\alpha(0)}(\mathcal{C})$ that generates the geodesic at $\alpha(0)$.

5 Experimental Results

In this section we describe some computer experiments for generating geodesic paths between shapes in $\mathcal{C}$. Let the two curves of interest be: $p_0(t) = (a\cos(t), b\sin(t), c\sqrt{b^2 - a^2\sin^2(t)})$, and $p_1(t) = (a(1+\cos(t)), \sin(t), 2\sin(t/2))$, and we want to compute a geodesic path between them in $\mathcal{C}$. Shown in Figure 3 are the

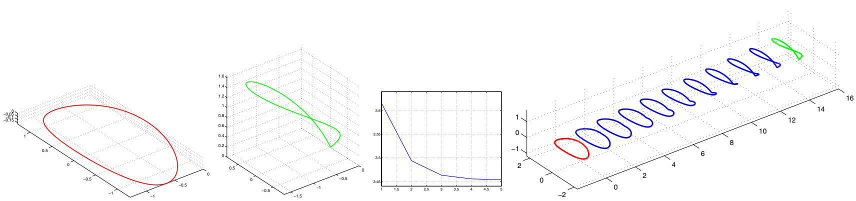

Fig. 3. The two shapes used in computing geodesic path, evolution of the energy E during path-straightening, and a view of that geodesic in $\mathbb{R}^3$

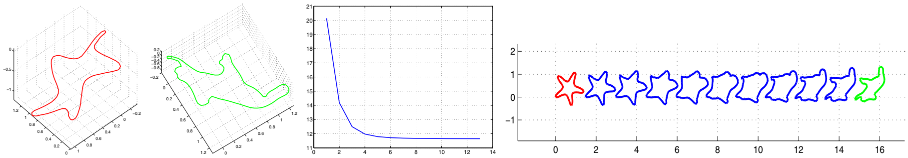

Fig. 4. Geodesic Computation: The two curves in $\mathcal{C}$, evolution of E as Algorithm 1 proceeds, and a view of the resulting geodesic path

results. The first two panels show the two curves. The first curve is an example of a *bicylinder* and the second one is an example of a *Viviani* curve. We apply Algorithm 1 on these two curves to generate a geodesic path between them. The third panel shows the evolution of the energy E during the iterations in Algorithm 1. The last panel shows a view of the resulting geodesic path in $\mathbb{R}^3$.

Shown in Figure 4 is another example, where the two end shapes (left two panels), evolution of the energy (middle), and a view of the final geodesic path (right) are displayed.

6 Summary

We have presented a differential geometric approach to studying shapes of closed curves in $\mathbb{R}^3$. The main tool presented in this study is the construction of geodesic paths between arbitrary two curves on an appropriate space of closed curves. This construction is based on path-straightening, i.e. we construct an initial path between those two curves, and iteratively straighten it using the gradient of the energy E. The limit point of this procedure is a geodesic path. We have presented step-by-step procedures for computing these geodesics, and have illustrated them using simple examples.

Acknowledgements

This research was supported in part by grants ARO W911NF-04-1-0268, ARO W911NF-04-1-0113, and CCF-0514743.

References

1. W. M. Boothby. *An Introduction to Differential Manifolds and Riemannian Geometry*. Academic Press, Inc., 1986.
2. A. M. Bronstein, M.M. Bronstein, and R. Kimmel. Three-dimensional face recognition. *International Journal of Computer Vision*, 64(1):5–30, 2005.
3. G. Dziuk, E. Kuwert, and R. Schatzle. Evolution of elastic curves in R^n: existence and computation. *SIAM J. Math. Anal*, 33:1228–1245, 2002.
4. J. P. Eakins, K. Shields, and J. Boardman. ARTISAN – a shape retrieval system based on boundary family indexing. In *Storage and Retrieval for Still Image and Video Databases IV. Proceedings SPIE*, volume 2670, pages 17–28, 1996.

5. U. Grenander and M. I. Miller. Computational anatomy: An emerging discipline. *Quarterly of Applied Mathematics*, LVI(4):617–694, 1998.
6. M. M. Kazhdan. *Shape Representations and Algorithms for 3D Model Retrieval.* PhD thesis, Computer Science, Princeton, April 2004.
7. E. Klassen and A. Srivastava. A path-straightening method for finding geodesics in shape spaces of closed curves in $\mathbb{R}^3$. *SIAM Journal of Applied Mathematics*, page in review, 2005.
8. E. Klassen, A. Srivastava, W. Mio, and S. Joshi. Analysis of planar shapes using geodesic paths on shape spaces. *IEEE Patt. Analysis and Machine Intell.*, 26(3):372–383, March, 2004.
9. J. Langer and D. A. Singer. Curve straightening and a minimax argument for closed elastic curves. *Topology*, 24:75–88, 1985.
10. J. Langer and D. A. Singer. Curve straightening in Riemannian manifolds. *Ann. Global Anal. Geom.*, 5:133–150, 1987.
11. P. W. Michor and D. Mumford. Riemannian geometries on spaces of plane curves. *Journal of the European Mathematical Society*, to appear, 2005.
12. W. Mio and A. Srivastava. Elastic string models for representation and analysis of planar shapes. In *Proc. of IEEE Computer Vision and Pattern Recognition*, 2004.
13. W. Mio, A. Srivastava, and E. Klassen. Interpolation by elastica in Euclidean spaces. *Quarterly of Applied Mathematics*, LXII(2):359–378, June 2004.
14. F. Mokhtarian, S. Abbasi, and J. Kittler. Efficient and robust shape retrieval by shape content through curvature scale space. In *Proceedings of First International Conference on Image Database and MultiSearch*, pages 35–42, 1996.
15. M. Novotni and R. Klein. A geometric approach to 3D object comparison. In *International Conference on Shape Modeling and Applications*, pages 167–175, 2001.
16. R. Osada, T. Funkhouser, B. Chazelle, and D. Dobkin. Matching 3D models with shape distributions. In *International Conference on Shape Modeling and Applications*, pages 154–166, 2001.
17. R. S. Palais. Morse theory on Hilbert manifolds. *Topology*, 2:299–340, 1963.
18. C. Samir, A. Srivastava, and M. Daoudi. Human face recognition using 2D facial curves. In *International Conference on Acoustic, Speech, and Signal Processing (ICASSP)*, May, 2006.
19. L. Younes. Optimal matching between shapes via elastic deformations. *Journal of Image and Vision Computing*, 17(5/6):381–389, 1999.